Journal of Physics: Conference Series

PAPER • **OPEN ACCESS**

Analysis of non-uniform residual stress state in plates with in-plane and transverse heterogeneities

To cite this article: R Nedin 2020 *J. Phys.: Conf. Ser.* **1479** 012119

Analysis of non-uniform residual stress state in plates with in-plane and transverse heterogeneities

R Nedin

I.I. Vorovich Institute of Mathematics, Mechanics and Computer Sciences, Southern Federal University, Rostov-on-Don, Russia

E-mail: rdn90@bk.ru

Abstract. In the present paper, we describe a model of a prestressed inhomogeneous body and provide the variational and weak statements. On its basis, we study a problem of mixed vibrations of a non-uniform plate with inclusions and a sandwich-structured three-ply plate under the conditions of the residual stress-strain state. We build the numerical finite-element solution on the basis of the weak problem statement and analyze the effect of the prestress states on its frequency response functions. In addition, we identify the prestress level in the middle layer of the composite plate by the data on frequency characteristics measurements.

1. Introduction

Investigations of problems on mechanics of deformable solid body under residual (or initial, or pre-) stress state play an important part in strength-and-stability assessment and in reconstruction of inhomogeneous properties [1]. In many works published, when modeling and identifying prestress state in the framework of nondestructive testing approach, authors use models of homogeneous prestresses. However, to provide efficient technologies of nondestructive testing, it is necessary to develop the models allowing to account and determine inhomogeneous prestress state on the basis of the given displacement or deformation fields at the body boundary with the usage of present-day computational algorithms including finite element method.

Among the works devoted to prestressed beams and plates, most of them relate to prestressed concrete and heterogeneous structures like sandwich composites. Problems on modern complex structural materials, for example, layered or functionally graded composites, in the presence of prestress fields, are scantly explored in the literature. In many engineering applications, researchers confine themselves to restoring magnitudes of initial forces forming prestress fields. In [2], the techniques for determining prestress in concrete structures are developed. The paper [3] presents a method for identifying pre-tension in a prestressed concrete bridge deck by measuring its dynamic responses; to simulate the bridge deck, the authors used the Euler-Bernoulli beam model and FEM. Inhomogeneous plates are common structural elements, therefore, their deformation models are extremely relevant in solving problems arising in modern construction, production of military and civilian technical systems of wide use (e.g. cutting systems, membrane sensors, shielding elements, etc.).

In manufacturing, residual stresses are often intentionally embedded in structures in order to improve their mechanical properties, e.g. formability. The article [4] presents computational and fullscale experiments to study the effect of elastic prestress on the deformed shape of an aluminum alloy plate sample at the stage of laser hardening. The authors proposed a new technique for simulating the effect of prestress on bending deformation and residual stress formation based on the "eigenstrain method" [5]. The numerical model allows predicting the deformed shape and uniaxial residual stress distributions in the plates under study.

We also note the importance of using variational and weak statements of direct and inverse problems allowing to describe operator relations and to provide efficient numerical solution. A new computational method for solving linear elasticity problems based on the combination of the Galerkin method and FEM is given in [6]. The idea behind the method lies in the use of weak statements for the corresponding differential operators.

A review of various approaches to modeling prestressed elastic bodies is given in [7]. In the work [8], a number of ways to identify prestress fields in elastic bodies, like plates, are described in the framework of non-destructive acoustic method. In [9-10], the problems of reconstructing an inhomogeneous prestressed state in non-uniform rods and thin plates are investigated, and some models of deforming prestressed plates within the classical approaches are proposed. Let us also mention the works [11,13] presenting a model of plate oscillations in the framework of non-classical deformation hypotheses and the technique for the inverse identification of plane prestressed state in a plate.

In this paper, on the basis of the model of a prestressed inhomogeneous body, we study mixed vibrations of a non-uniform plate with inclusions and a sandwich three-ply plate under the conditions of the residual stress-strain state, analyze the effect of the prestress states on its frequency response functions, and suggest a simple technique for identification of the prestress level in the composite plate by the data on the measured frequency characteristics.

2. Vibrations of a prestressed elastic body. Variational and weak formulations

Consider an elastic body in two configurations (see figure 1). In the initial deformed configuration κ_0, as a result of some finite deformations, a self-balanced field of initial stresses is present in the body. We shall consider this configuration as the reference one and use the material (Lagrangian) way of describing motion, i.e. relative to the coordinates of the position vector $\underline{R}_0$. Next, disturbing the configuration κ_0 and superimposing small deformations to it, we obtain the second configuration κ. We assume that in the configuration κ the body has a volume V bounded by the surface $S = S_u \cup S_\sigma$; it is rigidly clamped on the boundary part S_u, and it is loaded with a time-varying load $\underline{P}$ on the boundary part S_σ.

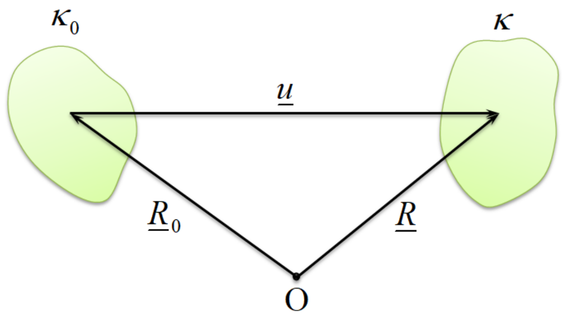

Figure 1. Two configurations of an elastic body: the initial one κ_0, and the perturbed one κ.

One of the most widespread models of prestressed bodies that can be found in literature is a model in which the initial deformed state can be determined by a geometrically linear theory. This assumption corresponds to the fact that the gradients of initial displacements can be neglected in comparison with unity. The linearized statement of the problem on steady-state oscillations of a prestressed elastic body for small incremental quantities without explicitly taking into account the initial deformation has the form [7,10,11]

$$T_{ji},_j + \rho b_i - \rho\omega^2 u_i = 0, \tag{1}$$

$$T_{ji} = \Gamma_{ji} + \sigma_{ij}, \quad \sigma^0_{ij},_j + \rho b^0_i = 0, \tag{2}$$

$$u^0_i \,|_{S^0_u} = f^0_i, \quad \sigma^0_{ij} n_j \Big|_{S^0_u} = P^0_i, \tag{3}$$

$$u_i \,|_{S_u} = 0, \quad T_{ji} n_j \Big|_{S_u} = P_i, \tag{4}$$

Here T_{ji} are the components of the nonsymmetric 1st Piola-Kirchhoff incremental stress, σ_{ij} are the components of the linearized symmetric 2nd Piola-Kirchhoff stress tensor, u_i are the small displacement vector components, ρ is the body density, b_i are the body force components, ω is steady-state vibration frequency, P_i are the components of the surface load vector. The quantities with the upper index "0" correspond to the initial body state (e.g., u_i^0 are the initial displacement vector components, σ^0_{mj} are the prestress tensor components, etc.). The incremental stress and strain tensors components are determined according to $\sigma_{ij} = C_{ijkl}\epsilon_{kl}$, $\epsilon_{ij} = \frac{1}{2}\left(u_{i,j} + u_{j,i}\right)$. Here $\Gamma_{ji} = u_{i,m}\sigma^0_{mj}$ are components of the tensor that generally depends on the prestress tensor components and the displacement gradient.

The variational and weak formulations of the problem (1)-(4) will take form

$$\int\limits_{S_\sigma} P_i \delta u_i d(S_\sigma) - \int\limits_V \sigma_{ij}\delta u_i,_j \, dV - \int\limits_V \Gamma_{ji}\delta u_i,_j \, dV + \omega^2 \int\limits_V \rho u_i \delta u_i dV = 0, \tag{5}$$

$$\int\limits_{S_\sigma} P_i v_i d(S_\sigma) - \int\limits_V \sigma_{ij}\epsilon^v_{ij} dV - \int\limits_V \Gamma_{ji} v_i,_j \, dV + \omega^2 \int\limits_V \rho u_i v_i dV = 0. \tag{6}$$

In [7] it was shown that the original oscillation problem reduces to the problem of finding the stationary value of the functional

$$\delta(\Pi + \Pi_0 - \omega^2 K) = 0 \tag{7}$$

$$\Pi = \tfrac{1}{2}\int\limits_V \sigma_{ij}\epsilon_{ij} dV - \int\limits_{S_\sigma} \underline{P}\cdot\underline{u} dS_\sigma, \quad \Pi_0 = \tfrac{1}{2}\int\limits_V \Gamma_{ji} v_i,_j \, dV, \quad K = \tfrac{1}{2}\int\limits_V \rho u_i^2 dV.$$

Here Π and K are classical representations for potential energy without taking into account prestress, and kinetic energy, respectively.

Such a formulation is convenient for solving a large class of inverse problems when it is required to determine the level or inhomogeneous prestress fields on the basis of the given information about the displacement field.

3. Problem for a prestressed plate with circular inclusions

Consider steady-state oscillations of an elastic isotropic inhomogeneous thin plate with a plane cross section S, clamped at the boundary part l_u, under the action of periodic uniformly distributed force $P = Pe^{i\omega t}$, applied to the boundary part l_σ. We assume that all the plate characteristics (ρ, h – the plate thickness, $\lambda = \dfrac{2\lambda^*\mu}{\lambda + 2\mu}$ – the Lamé parameter for the plane stress state, λ^* – the standard Lamé parameter, μ – the shear modulus) depend on 3 spatial coordinates. Suppose that the plate contains non-uniform spatial prestress distribution $\sigma^0_{ij} = \sigma^0_{ij}(x_k)$, $i, j, k = 1,2,3$. According to the plate theory in the framework of the Timoshenko-Mindlin model, and considering coupled in-plane and out-of-plane vibrations, we take on the following hypotheses

$$u_1 = \theta_1 x_3 + \zeta_1,\ \ u_2 = \theta_2 x_3 + \zeta_2,\ \ u_3 = w, \tag{8}$$

where $\theta_\alpha = \theta_\alpha(x_\beta)$ are the normal rotation angles along the axes x_α, $\zeta_\alpha = \zeta_\alpha(x_\beta)$ are in-plane displacements, $w = w(x_\beta)$ is the plate deflection, $\alpha, \beta = 1,2$. Denote the corresponding test functions by capital letters Θ_α, Z_α, W and assume they satisfy the same essential boundary as the functions θ_α, ζ_α, w do:

$$\Theta_\alpha\big|_{l_u} = 0,\ \mathrm{Z}_\alpha\big|_{l_u} = 0,\ W\big|_{l_u} = 0. \tag{9}$$

Based on hypotheses (8) and boundary conditions (9), the weak statement of the formulated problem (6) will take form [11]

$$\int_{l_\sigma}\left(P_\alpha Z_\alpha + P_3 W\right)dl - \int_S \Big\{Q_{\alpha\beta}\Theta_{\alpha,\beta} + R_{\alpha\beta}\mathrm{Z}_{\alpha,\beta} + S_\alpha\Theta_\alpha + T_\alpha W,_\alpha -$$
$$-\omega^2\left[\mathrm{P}_2\theta_\alpha\Theta_\alpha + \mathrm{P}_1\left(\theta_\alpha \mathrm{Z}_\alpha + \zeta_\alpha\Theta_\alpha\right) + \mathrm{P}_0\left(\zeta_\alpha \mathrm{Z}_\alpha + wW\right)\right]\Big\}dS = 0\,. \tag{10}$$

where

$$Q_{\alpha\beta} = \delta_{\alpha\beta}(\Lambda_2\theta_{m,m} + \Lambda_1\zeta_{m,m}) + \mathrm{M}_2(\theta_{\alpha,\beta} + \theta_{\beta,\alpha}) + \mathrm{M}_1(\zeta_{\alpha,\beta} + \zeta_{\beta,\alpha}) + \Sigma^2_{m\beta}\theta_{\alpha,m} + \Sigma^1_{m\beta}\zeta_{\alpha,m} + \Sigma^1_{\beta3}\theta_\alpha,$$

$$R_{\alpha\beta} = \delta_{\alpha\beta}(\Lambda_1\theta_{m,m} + \Lambda_0\zeta_{m,m}) + \mathrm{M}_1(\theta_{\alpha,\beta} + \theta_{\beta,\alpha}) + \mathrm{M}_0(\zeta_{\alpha,\beta} + \zeta_{\beta,\alpha}) + \Sigma^1_{m\beta}\theta_{\alpha,m} + \Sigma^0_{m\beta}\zeta_{\alpha,m} + \Sigma^0_{\beta3}\theta_\alpha,$$

$$S_\alpha = \mathrm{M}_0(w,_\alpha + \theta_\alpha) + \Sigma^1_{m3}\theta_{\alpha,m} + \Sigma^0_{m3}\zeta_{\alpha,m} + \Sigma^0_{33}\theta_\alpha,$$

$$T_\alpha = \mathrm{M}_0(w,_\alpha + \theta_\alpha) + \Sigma^0_{\alpha m}w,_m\,,$$

P_α are the in-plane components of the load vector, P_3 is the magnitude of the bending load.
Also we introduce the following functions:

$$G_p = \int_{-h/2}^{h/2} g x_3^p dx_3,\quad G_p = \left\{\Lambda_p, \mathrm{M}_p, \mathrm{P}_p, \Sigma^p_{\alpha\beta}\right\},\ \ g = \left\{\lambda, \mu, \rho, \sigma^0_{\alpha\beta}\right\}\ \ (\alpha, \beta, m = 1,2,\quad p = 0,1,2\,),$$

representing a generalization of the law for integral characteristics $\Lambda_p, \mathrm{M}_p, \mathrm{P}_p, \Sigma^p_{\alpha\beta}$ expressed through the corresponding parameters λ, μ, ρ, $\sigma^0_{\alpha\beta}$; for instance, $\Sigma^2_{12} = \int_{-h/2}^{h/2}\sigma^0_{12}x_3^2 dx_3$, $\mathrm{P}_1 = \int_{-h/2}^{h/2}\rho x_3 dx_3$.

Note that here we consider couple vibrations of the plate, including in-plane and out-of-plane modes. The problem in such a formulation can be divided and reduced to separate problem statements on in-plane and out-of-plane vibrations only if the additional symmetry conditions described in [11] are fulfilled. In the particular case for a plate with constant characteristics and a uniform prestress field, these conditions are met automatically, and the problem for the plate is successfully divided according to the oscillation modes. It is important that the proposed model allows you to set an initial state in the plate arbitrarily: both in the form of analytical dependencies and numerically.

It can be verified that, in a particular case for a homogeneous plate under conditions of a uniform prestressed state, if also the corresponding deformation conditions are fulfilled according to the

Kirchhoff model, the derived statement of the problem may be divided into two classical problems of bending and planar vibrations of the plate.

The problem (10) was studied numerically using the FEM; the influence of the inhomogeneous pre-stressed state plate on its amplitude-frequency characteristics and resonant frequencies was investigated.

Below, as an example, we provide the results of computational experiments of solving the direct problem for a prestressed rectangular plate with in-plane inhomogeneity: the plate made of fiberglass contains 4 circular aluminium inclusion (see figure 2). The problem parameters are as follows: $l = 1$ m (plate size along the axis x_1); $b = 0.4$ m (plate size along the axis x_2); $h = 0.05$m; the material of the plate fiberglass with the parameters $E_p = 35$ GPa, $\nu_p = 0.21$, $\rho_p = 1900\,\text{kg/m}^3$, the material of the inclusions is aluminium: $E_c = 170$ GPa, $\nu_c = 0.32$, $\rho_c = 2700\,\text{kg/m}^3$; the diameter of circular inclusions is $r_0 = 0.12b$.

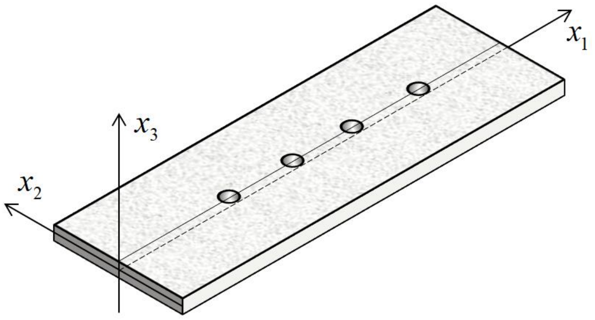

Figure 2. 3D view of the plate with circular inclusions.

The finite element mesh was additionally refined in the vicinity on the inclusions (figure 3). In all the figures below, the plate is clamped by the left side ($x_1 = 0$).

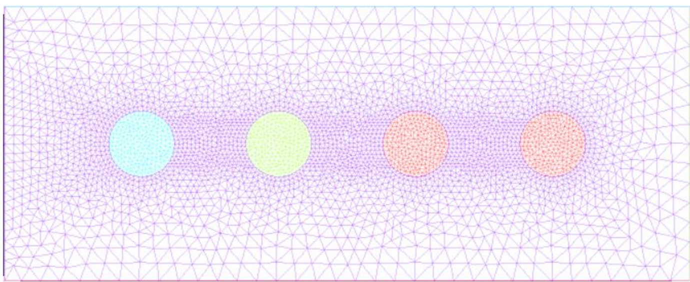

Figure 3. FE-mesh of the plate section 2D region.

As soon as we assume plate's thickness homogeneity, we have:

$$L_0(x_1,x_2) = \int_{-h/2}^{h/2} L(x_1,x_2)dx_3 = L(x_1,x_2)h, \quad L_1(x_1,x_2) = \int_{-h/2}^{h/2} L(x_1,x_2)x_3dx_3 = 0,$$

$$L_2(x_1,x_2) = \int_{-h/2}^{h/2} L(x_1,x_2)x_3^2dx_3 = \frac{1}{12}L(x_1,x_2)h^3,$$

where $L(x_1,x_2)$ stands for each material property ($E(x_1,x_2)$, $\nu(x_1,x_2)$, $\rho(x_1,x_2)$).

The non-uniform residual stress field is considered as a result of action of the initial mechanical load applied to the boundary part $P_1|_{x_1=l} = 150$ MPa (uniaxial pre-tension). To find such a field in the plate, the corresponding static problem was additionally solved, and the fields of initial displacements u_1^0, u_2^0 and stresses σ_{11}^0, σ_{12}^0, σ_{22}^0 were determined (see figure 4-5).

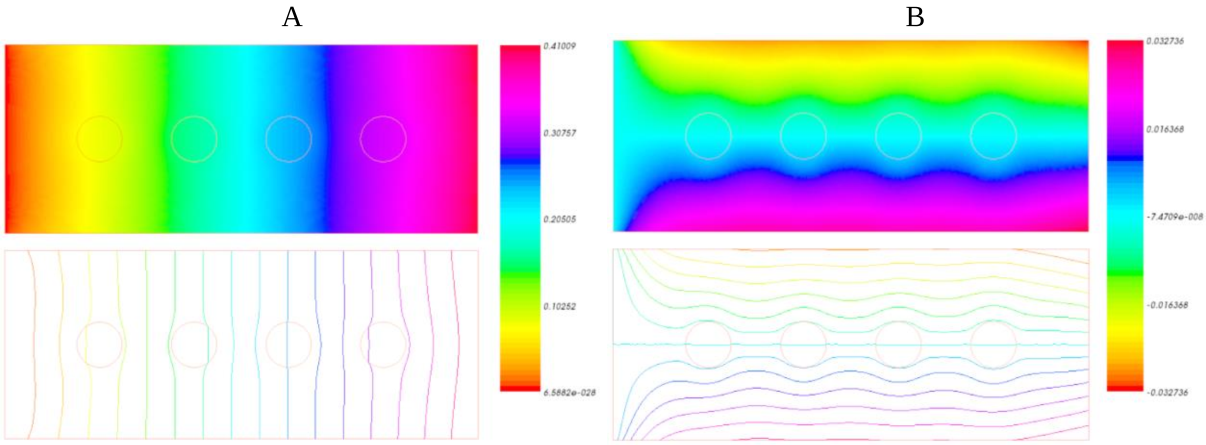

Figure 4. Results of the finite element calculation: initial displacement field (cm) u_1^0 (A), u_2^0 (B).

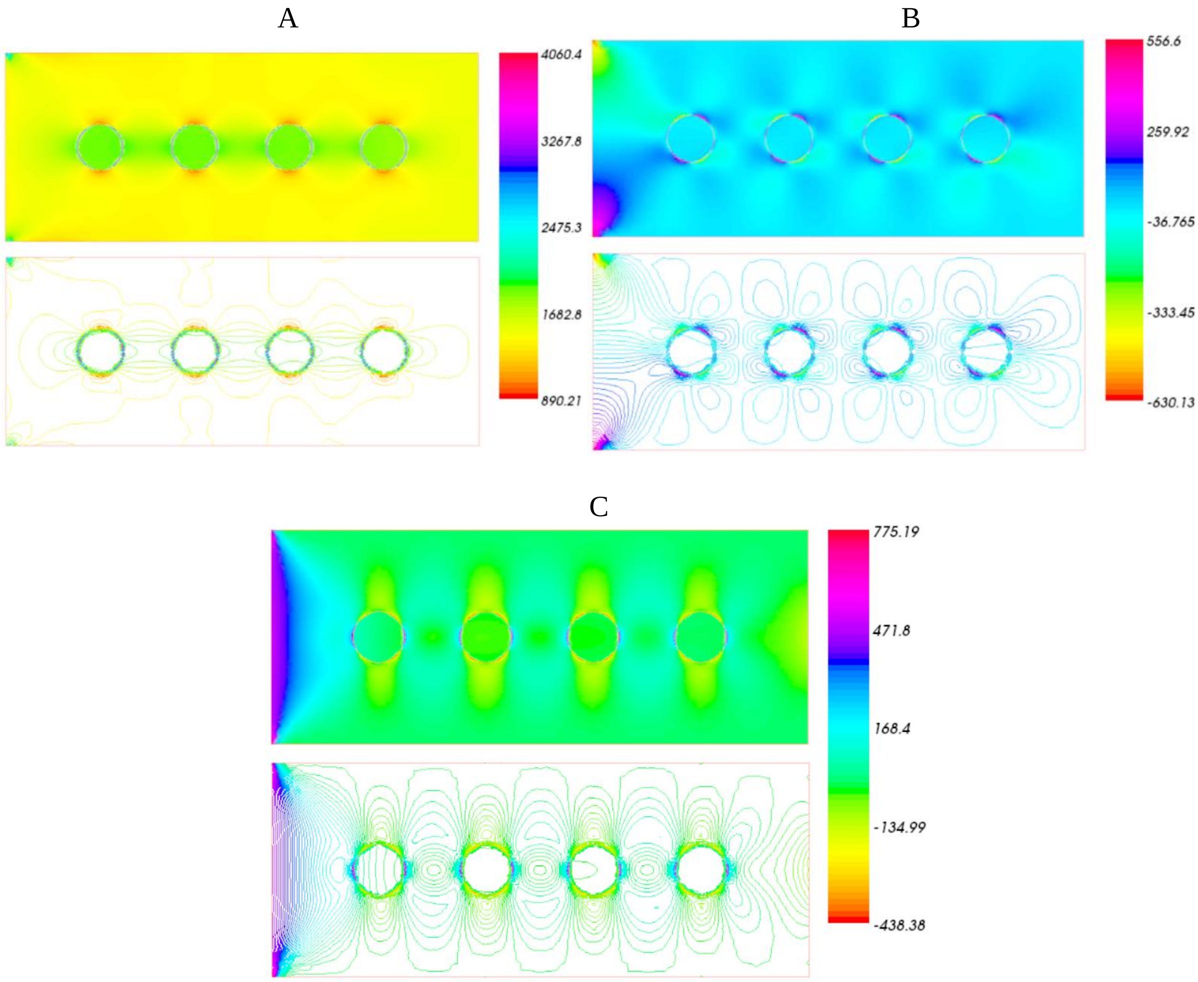

Figure 5. Results of the finite element calculation: prestress field (0.1 $\times$ MPa) σ_{11}^0 (A), σ_{12}^0 (B), σ_{22}^0 (C).

Figure 6 shows the fields of deflection and normal rotation angles calculated in the static case (for $\omega = 0$) for the plate taking into account the initial loading. The value of the bending load was equal to

IOP Conf. Series: Journal of Physics: Conf. Series **1479** (2020) 012119 doi:10.1088/1742-6596/1479/1/012119

$P_3 = -10$ MPa and was applied at the border $x_1 = l$. These functions were found as a result of solving the problem in its weak statement (10) (via FEM), with using the prestress functions σ_{11}^0, σ_{12}^0, σ_{22}^0 found numerically at the previous step.

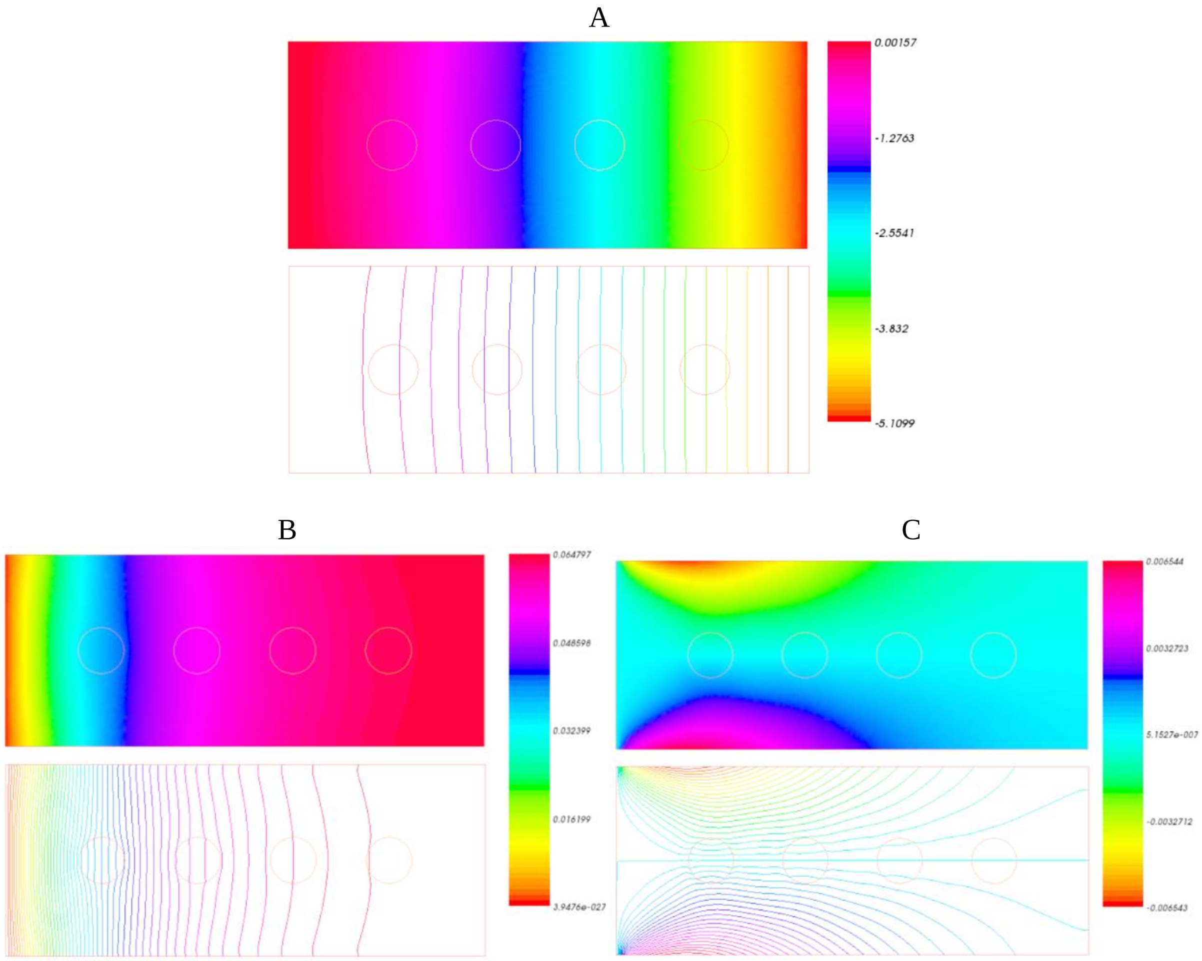

Figure 6. Results of the finite element calculation: A) deflection field w (cm); B) rotation angle θ_1 (dimensionless) field; C) rotation angle θ_2 (dimensionless) field.

Figure 7 shows the amplitude-frequency characteristics of the plate calculated at the point (l, 0) with and without prestress field. According to the curves obtained, it can be seen that the chosen inhomogeneous prestress field, formed as a result of applying a mechanical load, makes a significant contribution to the change of the amplitudes and the shift of resonant frequencies. Thus, it is permissible to consider an inverse problem on determination of level and structure of prestress state of a plate on the basis of the data on frequency response function measured in the resonance vicinity.

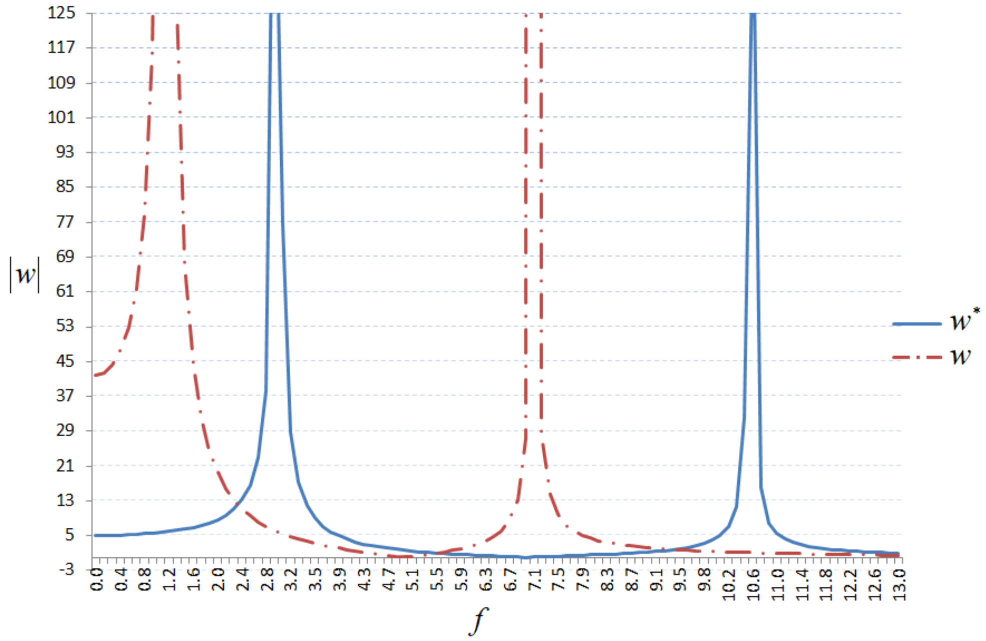

Figure 7. Frequency response function of the plate calculated at the point (l, 0) excluding (w) and taking into account the prestress field of (w^*).

4. Problem for a sandwich-structured composite prestressed plate

Now we consider a special problem for a three-ply sandwich plate with a uniformly prestressed (initially tensioned or compressed) inner layer of thickness δ (see figure 8).

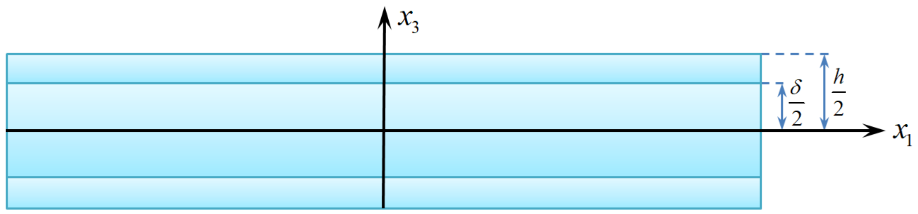

Figure 8. Cross section of the sandwich plate with a prestressed inner layer.

The material and prestress functions may be generalized as follows (figure 9):

$$L(x_3) = \begin{cases} L_2, & |x_3| \le \delta/2; \\ L_1, & |x_3| \in [\delta/2, h/2], \end{cases} \tag{11}$$

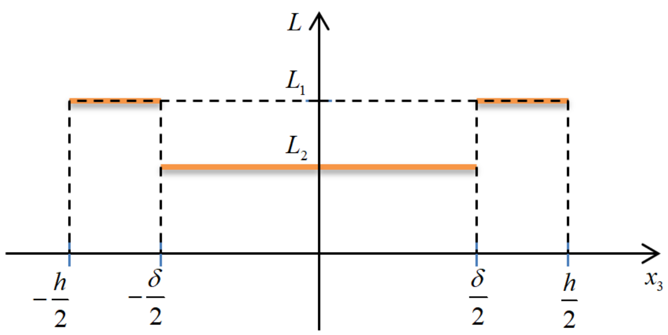

Figure 9. Material and prestress properties throughout the plate thickness.

Therefore,

$$L_0 = \int_{-h/2}^{h/2} L(x_3)dx_3 = L_2\delta - (h-\delta)L_1, \quad L_1 = \int_{-h/2}^{h/2} L(x_3)x_3 dx_3 = 0,$$

$$L_2 = \int_{-h/2}^{h/2} L(x_3)x_3^2 dx_3 = \frac{1}{12}L_2\delta^3 + \frac{1}{12}\left(h^3 - \delta^3\right)L_1, \tag{12}$$

Assume that the upper and lower layers are prestress free, and in the middle layer the prestress tensor component σ_{11}^0 is the only nonzero one: $\sigma_{11(1)}^0 = 0$, $\sigma_{11(2)}^0 = \sigma^0$. Hence,

$$\Sigma_{11}^0 = \int_{-h/2}^{h/2} \sigma_{11}^0 dx_3 = \sigma^0\delta, \;\; \Sigma_{11}^1 = \int_{-h/2}^{h/2} \sigma_{11}^0 x_3 dx_3 = 0, \;\; \Sigma_{11}^2 = \int_{-h/2}^{h/2} \sigma_{11}^0 x_3^2 dx_3 = \frac{1}{12}\sigma\,\delta^3, \tag{13}$$

In the same way as it was done with the previous problem, the problem for this plate was solved via FEM on the basis of the weak statement (10).

We also consider a problem of identifying the level of uniform prestressed state of the plate's middle layer. In this case, as the probing load, we choose the in-plane load applied to the free boundary part. The information on the plate geometry (the plate occupies rectangular continuous region), including the thickness of the middle layer, is considered known. In this case, after eliminating the part corresponding to the out-of-plane vibrations, the weak formulation (10) will take the form

$$\int_S \left(R_{11}\mathrm{Z}_{1,1} + R_{12}\mathrm{Z}_{1,2} + R_{21}\mathrm{Z}_{2,1} + R_{22}\mathrm{Z}_{2,2} - \omega^2\left[\mathrm{P}_0(\zeta_1\mathrm{Z}_1 + \zeta_2\mathrm{Z}_2)\right]\right)dS = -\int_{l_\sigma}\left(P_1 Z_1 + P_2 Z_2\right)dl$$

$$R_{11} = \Lambda_0\left(\zeta_{1,1} + \zeta_{2,2}\right) + 2\mathrm{M}_0\zeta_{1,1} + \Sigma_{11}^0\zeta_{1,1}, \;\; R_{22} = \Lambda_0\left(\zeta_{1,1} + \zeta_{2,2}\right) + 2\mathrm{M}_0\zeta_{2,2}$$

$$R_{12} = \mathrm{M}_0(\zeta_{1,2} + \zeta_{2,1}), \;\; R_{21} = \mathrm{M}_0(\zeta_{1,2} + \zeta_{2,1}) + \Sigma_{11}^0\zeta_{2,1}, \tag{14}$$

In this particular case, the formulation (14) includes only the integral characteristics corresponding to the common averaging according to the theory of the mean value of a function: characteristics of elastic modules Λ_0, M_0 and of prestress component Σ_{11}^0. Thus, we can express the integral characteristic Σ_{11}^0 through other known integral characteristics and the planar displacement field from the weak formulation of the direct problem (14), or from the similar formulation of the boundary value problem [10]. Based on the result published in [13] and taking into account that $\sigma^0 = \Sigma_{11}^0/\delta$, we obtain

$$\sigma^0 = -\tfrac{h}{\delta}\left[\left(\Lambda_0\left(\zeta_{1,1} + \zeta_{2,2}\right) + 2\mathrm{M}_0\zeta_{1,1}\right)_{,1} + \mathrm{M}_0(\zeta_{1,2} + \zeta_{2,1})_{,2}\right]/\,\zeta_{1,11}. \tag{15}$$

The formula (15) allows to restore the value σ^0 based on the additional information on the given values of the components of planar displacements ζ_1, ζ_2 measured in a set of points in the sectional area of the plate S for a given oscillation frequency. Using, for example, the spline interpolation, one may calculate the functions of displacement ζ_1, ζ_2 based on their values in the points set, and then find the derivatives $\zeta_{i,j}$ with the help of these functions at the required points of the plate.

In order to restore various values of the prestressed state level of the middle layer, we conducted a series of computational experiments; we considered the range $\sigma^0 / E_1 = 10^{-5} \div 10^{-2}$ for different frequencies from the frequency range below the 2nd resonance. The plate parameters are as follows: $l = 0.2\,\text{m}$, $b = 0.05\,\text{m}$, $h = 0.003\,\text{m}$, $\delta = 0.4h$, $\nu_p = \nu_c = 0.29$, $E_1 = 210\,\text{GPa}$, $\rho_1 = 7700\,\text{kg/m}^3$, $E_2 = 300\,\text{GPa}$, $\rho_2 = 9000\,\text{kg/m}^3$. To calculate the solution of the corresponding direct problem, we used a uniform 80 × 60 finite element mesh. The analysis of numerical experiments on the level σ^0 reconstruction revealed that the accuracy of the inverse problem solution largely depends on the choice of the probing frequency and the loading mode. Table 1 shows some results of the reconstruction of σ^0 under the longitudinal uniformly distributed vibratory load (along the axis x_1) applied to the free face of the plate, at a frequency of 223.985 Hz (in the vicinity of the first longitudinal resonance).

Table 1. Results of the reconstruction error of the middle layer prestress level (the exact value σ^0 and the reconstruction $\tilde{\sigma}^0$ were compared).

Prestress level $\tau = \sigma^0 / E_1$	Relative reconstruction error (%)
10^{-6}	91.0898
10^{-5}	8.187
10^{-4}	0.102991
10^{-3}	0.931623
10^{-2}	1.00991

It can be seen from the table that the reconstruction is successful for the prestress levels exceeding the value $\tau = \sigma^0 / E_1 = 10^{-5}$; lower prestress levels do not have any significant frequency response, and therefore their recovery process is difficult. Let us mention that for the series of experiments described above, the most advantageous ranges for selecting the probe frequency were located in a close vicinity of the first longitudinal resonance frequency. In this way, this result correlates to the results published in [13]. In addition, let us mention a directly proportional dependency of the reconstruction accuracy on the middle ply thickness.

Acknowledgments
This study was supported by the Russian Science Foundation (project No. 18-71-10045).

References

[1] Rossini N, Dassisti M, Benyounis K and Olabi A 2012 Materials & Design **35** 572–588
[2] Bagge N, Nilimaa J and Elfgren L 2017 Engineering Structures **135** 41–52
[3] Lu Z and Law S 2006 Mechanical Systems and Signal Processing **20** 2186–2199
[4] Hua Y, Li Z, Yu X and Yao Z 2015 J. Materials Processing Technology **221** 214–224
[5] Korsunsky A 2006 J. Strain Anal. Eng. **41** 195–204
[6] Wang C, Wang J, Wang R and Zhang R 2016 J. Computational and Applied Mathematics **307** 346–366
[7] Nedin R, Dudarev V and Vatulyan A 2017 Engineering Structures **151** 391–405
[8] Dudarev V, Nedin R and Vatulyan A 2014 Advanced Materials Research **996** 409–414

[9] Nedin R and Vatulyan A 2014 ZAMM **94**(1) 142–149
[10] Nedin R and Vatulyan A 2013 International Journal of Solids and Structures **50** 2107–2114
[11] Nedin R, Vatulyan A and Bogachev I 2017 Mathematical Methods in the Applied Sciences **41**(4)1600–1618
[12] Nedin R and Vatulyan A 2011 Advanced Structured Materials **13** 165–182
[13] Vatulyan A, Nedin R and Dudarev V 2019 IOP Conf. Series: Journal of Physics: Conf. Series **1203** 012027